Polymer 51 (2010) 249–256

Contents lists available at ScienceDirect

Polymer

journal homepage: www.elsevier.com/locate/polymer

Effects of ultrasound on the conformation and crystallization behavior of isotactic polypropylene and β-isotactic polypropylene

Jian Kang, Jinyao Chen, Ya Cao, Huilin Li*

State Key Laboratory of Polymer Materials Engineering, Polymer Research Institute of Sichuan University, Chengdu, Sichuan 610065, People's Republic of China

ARTICLE INFO

Article history:
Received 17 April 2009
Received in revised form
21 September 2009
Accepted 3 November 2009
Available online 17 November 2009

Keywords:
Ultrasound
Polypropylene conformation
Memory effect

ABSTRACT

The effects of ultrasonic irradiation on conformation and crystalline structure of isotactic polypropylene (iPP) and β-isotactic polypropylene (β-iPP) were studied by means of Fourier transform infrared spectroscopy (FT-IR), differential scanning calorimetry (DSC) and wide-angle X-ray diffraction (WAXD). The results demonstrate that ultrasonic irradiation decreases the helical conformation order and changes the crystalline structures: for iPP, T_m and T_{onset} decrease, $T_m - T_{onset}$ becomes larger; for β-iPP, the β_c, $(1-\lambda)_\beta$ and k_β increase, the intensities of α(040) plane and α(130) plane in WAXD profiles decrease evidently. For both iPP and β-iPP, the crystallinity decreases, *d*-spacing increases, the crystallite size *L* decreases and ultrasound shows a selective effect on the growth of β-crystal. Furthermore, DSC and WAXD were employed to observe the effect of ultrasound on the "melting memory effect" of β-iPP. The results indicate that ultrasonic irradiation destructs the existing "locally ordered structure" in β-iPP melt, as a result greatly inhibits the βα-recrystallization of β-iPP samples during heating.

1. Introduction

Ultrasound is one sort of elastic mechanic wave in the frequency range of 10^4–10^8 Hz. The application of ultrasonic in polymer processing is attractive because it can accelerate chemical reactions, modify the rheological and mechanical properties, and so on. Isayev et al. studied the processing of polymers using high-power ultrasound and the results indicated that ultrasonic vibration during extrusion modified the die characteristics [1–4]. By introducing ultrasonic vibration into an extruder, they studied the process of recycling rubber waste [5,6]. In solidifying polymer, the crystalline structure formed can be well controlled by introducing ultrasonic energy [7]. Khamad and coworkers studied the extrusion process of HDPE containing a small amount of butyl rubber under ultrasonic irradiation and found that the crystallinity increases, the structural defects are reduced and the mechanical properties are enhanced [8].

FT-IR spectroscopy, which is sensitive to the constitution and the folding manner of iPP molecular chains, is an effective method for characterizing the changes of helical conformation of iPP [9–11]. During the past decade, the relationship between specific regularity bands of FT-IR spectrum and the different critical helix length "*n*" of iPP had been well established [12–19]. The IR bands at 940, 1220, 1167, 1303, 1330, 840, 998, 900, 808, 1100, and 973 cm^{-1} correspond to helical structures with degree of order from high to low, and the minimum *n* values for appearance of bands at 973, 998, 840 and 1220 cm^{-1} are 5, 10, 12 and 14 monomers units in helical sequences, respectively. Apparently, the larger the *n* value is, the higher the ordered degree of the corresponding regularity is. Therefore, the information of conformational changes of iPP and β-iPP after ultrasonic irradiation can be obtained by calculating the absorbance variations of these regularity bands in FT-IR spectra. In the present work, the intensities of four strongest bands at 973, 998, 840 and 1167 cm^{-1}, corresponding to helical sequences with 2–4, 5–10, 12–14, and 14 or more monomer units respectively, are calculated to measure the influence of ultrasonic irradiation on conformation of iPP and β-iPP.

The phase transformation during heating from metastable β-phase to stable α-phase is a characteristic feature of β-iPP and had been extensively investigated [20–34]. The βα-recrystallization during heating of β-iPP is due to the melting memory effect, which is quite sensitive to the post-crystallization thermal history of the samples, for it is added onto the driving force only if the sample is cooled below a critical temperature, namely, T^*_R (i.e. 100–105 °C) [25,30,35,36]. One explanation for the melting memory effect of β-iPP is that there exists some "locally ordered structure" within iPP melt, which can hardly be removed even when samples are heated to 200 °C. After the melt is cooled below T^*_R, due to the stereo regularity induced by the existence of "locally ordered structure", a very small amount of finely

* Corresponding author. Tel.: +86 028 85406333; fax: +86 028 85402465.
E-mail address: nic7703@scu.edu.cn (H. Li).

0032-3861/$ – see front matter © 2009 Elsevier Ltd. All rights reserved.
doi:10.1016/j.polymer.2009.11.018

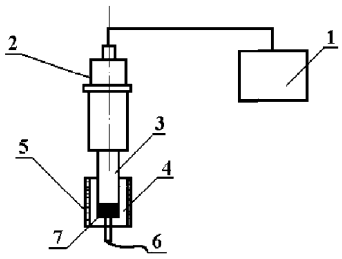

1,Ultrasonic generator, 2,Piezoelectric transducer, 3,Horn, 4,Die,

5,Electric heaters, 6,Thermocouple, 7,Melt

Scheme 1. Scheme of static ultrasonic wave system.

dispersed α-nuclei within the β-phase is formed due to a self-nucleation process. When the samples are reheated, this α-nuclei can induce a $\beta\alpha$-recrystallization process in the partial melting of the β-phase [37,38]. However, compared with the α-phase directly formed during the primary crystallization or due to the $\beta\alpha$-recrystallization when recooled samples are heated, the amount of the dispersed α-nuclei is very small and can hardly be normally detected by X-ray diffraction [30]. It is worth noting that the simultaneous DSC and WAXD study of Hiroki Uehara et al. [39] delivered useful information, which is helpful for a better understanding of the DSC thermograms for β-iPP. However, little work has been focused on the influence of ultrasonic irradiation on conformational aspect of iPP and β-iPP. On the other hand, the changes of crystalline structure and melting behavior of β-iPP under ultrasonic irradiation are still unknown.

Our previous works [40,41] studied the influences of ultrasound on processing and structure of iPP during extrusion, and on crystalline structure of nucleated iPP within a static ultrasonic wave system. This work focuses on the effect of ultrasonic irradiation on conformation, crystalline structure and melting behavior of iPP and β-iPP nucleated by β-nucleating agent (designated as β-iPP in this paper) under static ultrasonic irradiation. Changes on conformation and crystalline structure after ultrasonic irradiation are discussed. Furthermore, the influence of ultrasound on the "melting memory effect" of β-iPP is studied and the corresponding mechanism is discussed.

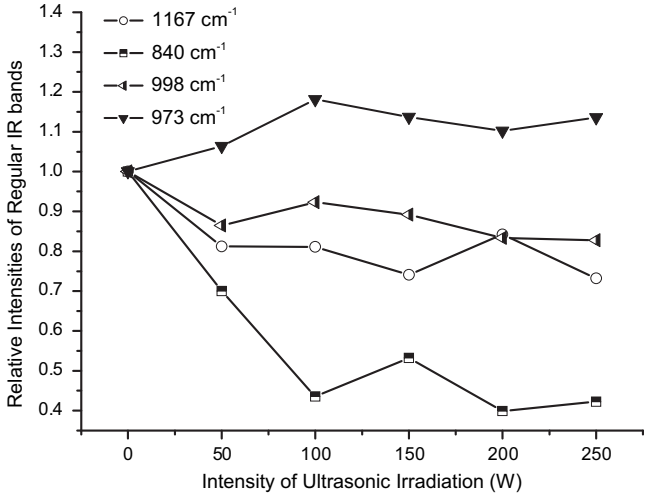

Fig. 1. Intensity variation of different regularity bands of iPP samples, as a function of the ultrasound intensity. The intensity of all the bands at 0 W was taken as the reference.

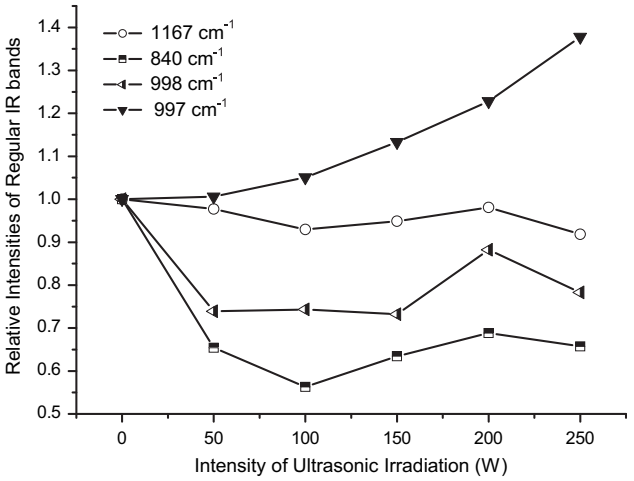

Fig. 2. Intensity variation of different regularity bands of β-iPP samples, as a function of the ultrasound intensity. The intensity of all the bands at 0 W was taken as the reference.

2. Experimental section

2.1. Materials and sample preparation

The isotactic polypropylene (iPP), grade T30s, with a melt flow index (MFI) of 2.5 g/10 min and number average molecular weight (M_n) of 2.8×10^5, was produced by Dushanzi Petrochemical Corporation (China). The β-nucleating agent was a powder of *N*,*N*′-dicyclohexyl-2,6-naphthalenedicarboxamide (DCNDCA, trade name TMB-5) purchased from Shanxi Chemical Academe and was used as received.

Scheme 1 shows the static ultrasound experimental equipment consisting of a mold and an ultrasonic generator. The frequency of ultrasound is 20 kHz and power ranges from 0 to 300 W; the diameter of the horn is 15 mm.

The β-iPP samples studied in this paper were prepared with β-nucleating agent TMB-5. The iPP pellets and TMB-5 were first mixed in the weight ratio of 100:2 and then extruded by a twin-screw extruder (SHJ-20, Nanjing Giant Machinery Co., Ltd, the screw speed is 10 rpm and the temperature of each part is 175, 185, 190, 190 °C, respectively) and pelletized to obtain a master batch. The master batch and iPP were mixed and extruded by twin-screw

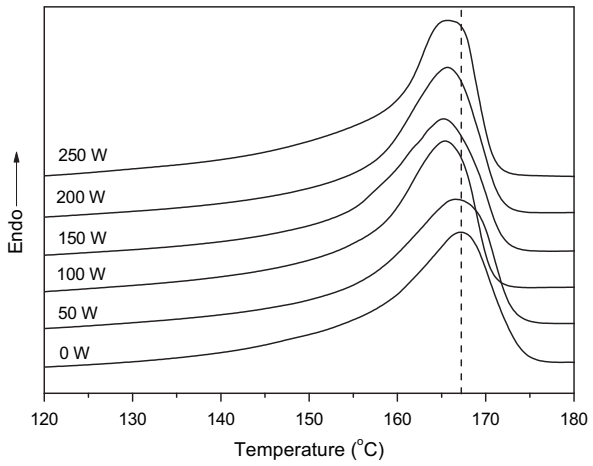

Fig. 3. The DSC heating thermograms of iPP samples under different intensities of ultrasonic irradiation.

Table 1
Melting parameters of iPP under different intensities of ultrasonic irradiation.

Ultrasound intensity (W)	Crystallinity (%)	T_m (°C)	T_{onset} (°C)	$T_m - T_{onset}$ (°C)
0	57.6	167.7	156.5	11.2
50	52.9	167.0	154.6	12.4
100	52.2	166.3	153.3	13.0
150	51.4	165.2	153.0	12.2
200	53.1	165.8	151.9	13.9
250	52.6	165.5	153.2	12.3

again to obtain β-iPP pellets. The concentration of nucleating agent was 0.3 wt%.

The iPP pellets and β-iPP pellets were respectively melted in the static ultrasonic mold for 12 min and then irradiated by ultrasonic wave (at 0, 50, 100, 150, 200, 250 W intensities) for 3 min. The temperature was controlled at 190 ± 1 °C throughout the process. After that, they were cooled to room temperature and characterized.

2.2. Characterization

2.2.1. FT-IR

All samples were cut into thin film of 10 μm (in thickness) by a microtome. The spectra were measured at 26 °C using a Nicolet Magna 560 FT-IR spectrometer in ATR method. The spectra were collected at a resolution of 4 cm^{-1} with 16 scans. The range of measured wavenumber was 400–4000 cm^{-1}. All the original spectra were baseline corrected using OMNIC E.S.P software.

2.2.2. DSC

The calorimetric measurements were carried out on a Mettler Toledo DSC1 differential scanning calorimeter. Before the measurements, temperature was calibrated by using Indium as a standard medium. Measurements were performed with the samples of 4–5 mg at a standard heating rate of 10 °C/min under constant nitrogen flow starting from 50 to 200 °C. All the thermograms were fitted and the β-fraction (β_c) was estimated from DSC by the following expression [42]:

$$\beta_c = (1-\lambda)_\beta / \left[(1-\lambda)_\beta + (1-\lambda)_\alpha\right]$$

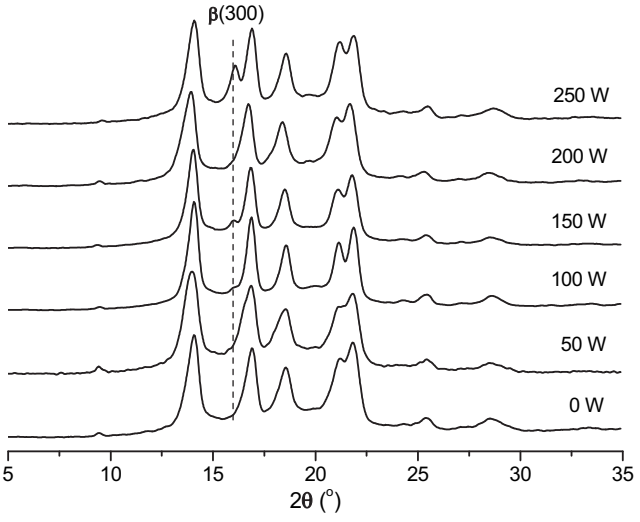

Fig. 4. WAXD profiles of iPP under different intensities of ultrasonic irradiation.

The degree of crystallinity ($1-\lambda$) associated with each phase was calculated from the ratio ΔHα/ΔHu. ΔHα and ΔHu are the apparent and completely crystalline heats of fusion, respectively, and the values used for ΔHu for 100% crystalline α-iPP, 100% crystalline β-iPP and the 100% crystalline iPP were 177.0, 168.5 and 209 J g^{-1}, respectively [23,43].

2.2.3. WAXD

All WAXD experiments were performed with a DX-1000 diffractometer. The wavelength of CuKα was $\lambda = 0.154$ nm and the spectra were recorded in the 2θ range of 5–35°, a scanning rate of 2°/min, and a scanning step of 0.02°. The crystallite size L of each plane of samples was determined from the XRD using the Debye–Scherrer's equation [44]:

$$L = 0.9\lambda/\beta \cos\theta$$

where λ is the X-ray wavelength of radiation used, θ is the Bragg angle and β is the full width of the diffraction line at half maximum (FWHM) intensity measured in radians.

The content of the β-crystal form was determined according to standard procedures described in the literature [23], employing the following relation:

$$k_\beta = \frac{H_\beta(300)}{H_\beta(300) + H_\alpha(110) + H_\alpha(040) + H_\alpha(130)}$$

k_β denotes the relative content of β-crystal form (WAXD), $H_\alpha(110)$, $H_\alpha(040)$ and $H_\alpha(130)$ are the intensities of the strongest peaks of α-form attributed to the (110), (040) and (130) planes of monoclinic cell, respectively. $H_\beta(300)$ is the intensity of the strongest (300) diffraction peak of the trigonal β-form.

3. Results and discussion

3.1. Effect of ultrasonic irradiation on conformation of iPP and β-iPP

Each IR band has its own intensity coefficient, as a result, it is necessary for the intensities of these regular helical conformation bands to be normalized. The IR band at 1460 cm^{-1}, which corresponds to the asymmetric deformation vibration of the methyl group, can serve as an internal standard because it is almost not influenced by the variation of external environment [10,11,45]. The normalized intensity variation of the different regularity bands of iPP and β-iPP samples with (50, 100, 150, 200, 250 W samples) and without (0 W sample) ultrasonic irradiation, calculated from the IR spectra, are shown in Figs. 1 and 2, respectively, as a function of ultrasonic intensity. The intensity of all the bands at 0 W was taken as the reference.

Figs. 1 and 2 show that the trends for the intensity variation of each regularity bands of iPP and β-iPP samples are similar. Compared with sample without ultrasonic irradiation, the intensities of different regularity bands at 973, 998, 840, 1167 cm^{-1} changed greatly with ultrasonic irradiation. The trends for the intensity variation of different regularity bands are quite different: the intensities of 998, 840, 1167 cm^{-1} bands, corresponding to helical sequences with more than 5 monomer units, decrease while the intensity of 973 cm^{-1} band with 2–4 monomer units increases. Especially, different regularity bands have different response to ultrasound, the intensity of 840 cm^{-1} band with 12 monomer units decreases faster than that of 1167 and 998 cm^{-1} bands, implying that the 840 cm^{-1} band with 12 monomer units is more sensitive to ultrasonic irradiation among these regularity bands.

The above intensity variations indicate that when ultrasound is applied in iPP and β-iPP melt, the molecular movement becomes

Table 2
WAXD parameters of iPP under different intensities of ultrasonic irradiation.

Ul intensity (W)	k_β(%)	*d*-spacing (angstrom)				*L*(nm)			
		$(110)_\alpha$	$(040)_\alpha$	$(130)_\alpha$	$(300)_\beta$	$(110)_\alpha$	$(040)_\alpha$	$(130)_\alpha$	$(300)_\beta$
0	–	6.278	5.246	4.784	–	14.1	16.8	15.7	–
50	–	6.321	5.249	4.792	–	10.5	11.9	11.4	–
100	1.0	6.293	5.247	4.777	5.539	11.9	14.1	12.7	14.1
150	7.94	6.302	5.253	4.801	5.546	14.0	15.8	14.8	9.8
200	–	6.365	5.298	4.818	–	11.0	13.7	11.8	–
250	11.1	6.379	5.302	4.834	5.568	11.2	13.0	11.6	9.6

more intensive, the molecular entanglement is reduced. During the cooling process, the content of helical conformation with shorter monomer units increases while the content of helical sequences with longer ones decreases, it is preferable for molecules to fold into the shorter helical sequences with less than 5 monomer units. In general, the helical conformation order of iPP and β-iPP macromolecules decreases under ultrasonic irradiation.

3.2. Effect of ultrasound on crystalline structure of iPP

Fig. 3 shows the DSC heating thermograms of iPP under different intensities of ultrasonic irradiation, and Table 1 summarizes the corresponding thermal data obtained from Fig. 3. T_m is the melting peak temperature, T_{onset} is the initial melting temperature and $T_m - T_{onset}$ is an evaluation standard of the crystalline perfection of polymer. The larger $T_m - T_{onset}$ is, the wider the distribution range of the crystalline perfection is.

As can be seen from Fig. 3 and Table 1, after ultrasonic irradiation, the melting curves shift to lower temperature region, meanwhile, the crystallinity decreases, both T_m and T_{onset} decrease, $T_m - T_{onset}$ becomes larger. All these results indicate that ultrasonic treatment induces a decrease in the degree of crystalline perfection and a wider distribution range of the crystalline perfection of iPP.

As is shown in the X-ray diffraction profiles (Fig. 4), after ultrasonic irradiation, the peak at $\theta = 16°$, characteristic of $\beta(300)$ plane, emerges under 100, 150 and 250 W intensities, indicating the formation of β-crystal after ultrasonic treatment. The above results indicate that it is preferable for the formation of β-crystal in iPP rather than that of α-crystal under ultrasonic treatment. Moreover, the corresponding WAXD parameters listed in Table 2 show that nearly all *d*-spacing of crystal planes of iPP increase and crystallite size *L* decreases with ultrasonic irradiation, indicating that the crystal particles pack looser and the crystallite size decreases.

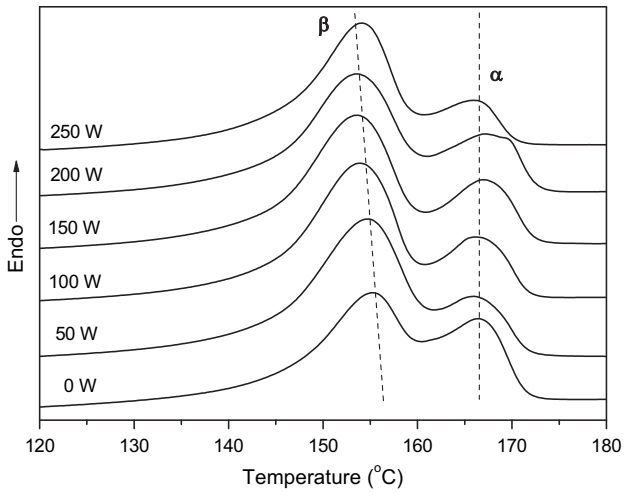

Fig. 5. DSC heating thermograms of β-iPP under different intensities of ultrasonic irradiation.

3.3. Effect of ultrasound on crystalline structure of β-iPP

Fig. 5 shows the DSC heating thermograms of β-iPP, and the parameters calculated from Fig. 5 are listed in Table 3. Attributed to the dual nucleation ability of TMB-5 [46], the melting peak of α-phase is observed in all the heating thermograms of related samples. Moreover, the relative content of β-fraction (βc) and the crystallinity of β-crystal $(1 - \lambda)_\beta$ increase, and the crystallinity of β-iPP decreases prominently. These results imply that ultrasonic irradiation decreases the crystalline perfection and makes the distribution range of the crystalline perfection of β-iPP wider. On the other hand, for β-iPP nucleated by DCNDCA, ultrasound shows a selective effect on the growth of different crystal forms, which encourages the growth of β-crystal.

It is worth noting from the WAXD profiles and parameters (Fig. 6 and Table 4) that, the diffraction peak at $\theta = 16.0°$, characteristic of β (300) plane, becomes evidently sharper after ultrasonic irradiation; meanwhile, the intensities of the diffraction peaks at $\theta = 16.9°$ and 18.5°, corresponding to α (040) plane and α (130) plane, decrease obviously, and the intensity of the diffraction peak at $\theta = 14.1°$ corresponding to the α (110) plane remains constant. This implies that after ultrasonic irradiation, iPP melt tends to crystallize into β-modification rather than α-phase, and the growth of α (040) and α (130) plane are restrained. It is coincident with the DSC analysis and further proves that ultrasound is an effective method to enhance content of β-crystal. On the other hand, the increase in the *d*-spacing indicates that the crystal packs looser and the decrease of *L* indicates a decrease in the crystallite size.

The above results demonstrate that ultrasonic irradiation can induce a reduction of helical conformation order in iPP and β-iPP samples, decrease the crystalline perfection, and widen the distribution range of the crystalline perfection. Two possible mechanisms might explain the relationship between conformational changes and crystalline structural changes: one possibility involves the memory effect during crystallization process due to the ordered structures within polymer melts [21,47,48]. During crystallizing from melts, the remained ordered structures can act as nucleation precursors for polymer crystallization and subsequently influence the crystallization rate and morphology. The lower the degree of order in melts, the more the free energy difference between crystalline regions and melts, resulting in a harder occurrence of crystallization [17,49]. Since the degrees of conformational order in iPP and β-iPP melts are decreased under ultrasonic irradiation, it might be more difficult for iPP molecules

Table 3
Melting parameters of β-iPP under different intensities of ultrasonic irradiation.

Ultrasound intensity (W)	Crystallinity of β-iPP (%)	$T_{\beta\text{-peak}}$ (°C)	β_c (%)	$(1 - \lambda)_\beta$ (%)	$(1 - \lambda)_\alpha$ (%)
0	57.9	157.5	72.4	51.3	19.6
50	55.3	154.9	83.8	57.3	11.1
100	54.1	153.8	80.4	53.7	13.1
150	53.4	153.5	78.4	52.0	14.3
200	52.6	153.3	78.6	51.4	14.0
250	52.6	154.1	79.1	51.6	13.0

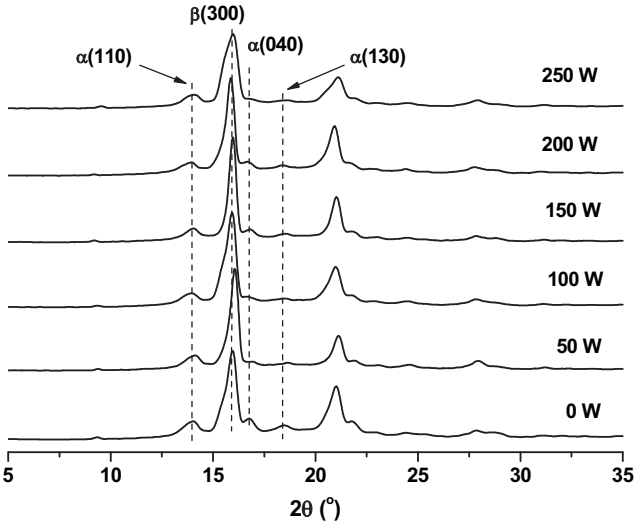

Fig. 6. WAXD profiles of β-iPP under different intensities of ultrasonic irradiation.

to crystallize, and then the primary nucleating rate and morphology are modified, finally the crystallinity and crystal perfection are decreased. Another possibility relates to the study of characteristic conformational changes during crystallization process. The studies of Zhu X.Y et al.[19] confirmed that iPP melt system will be stable when the persistence length of 3_1 helical sequences is less than 12 monomer units. As soon as the helix length exceeds 12 monomer units, corresponding to the emergence of regularity band at 840 cm^{-1}, the 3_1 helix conformation extends quickly and then crystallization occurs. Interestingly, the results of our work indicate that the regularity band at 840 cm^{-1} with 12 monomer units is most sensitive to ultrasonic irradiation and decreases most drastically after crystallization is accomplished. After ultrasonic irradiation, the formation of helical sequences with 12 monomer units is drastically inhibited, which might subsequently make the occurrence of crystallization harder and finally modify the crystallization behavior of iPP and β-iPP.

In general, all the FT-IR, DSC and WAXD analysis above suggest that ultrasound disorders the helical conformation order of iPP and β-iPP melts, thus changing the melting behavior and crystalline structure.

13.4. Effect of ultrasonic irradiation on "melting memory effect" of β-iPP

Now we come to the effect of ultrasound on the "melting memory effect" of β-iPP.

Figs. 7 and 8 give the DSC, WAXD profiles of β-iPP samples newly prepared (a) and 28 days after preparation (b), respectively. As can be seen from Fig. 7a, when samples are newly prepared, the melting peaks of α- and β-phase emerge at about 167 °C and 154 °C,

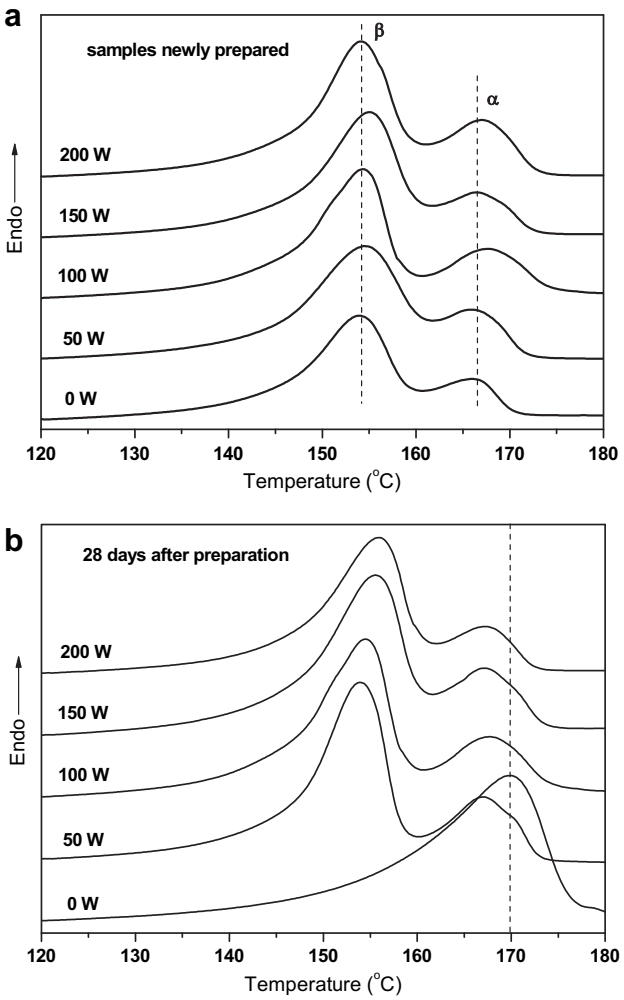

Fig. 7. (a) DSC curves of β-iPP samples newly prepared. (b) DSC curves of β-iPP samples cooled under room temperature 28 days after preparation.

respectively, indicating that the α- and β-phase of all samples melt separately; however, 28 days later (Fig. 7b), for sample without ultrasonic treatment (0 W), the melting peak of β-phase vanishes and the melting peak of α-phase shifts to higher temperature; on the other hand, for samples with ultrasonic treatment (50, 100, 150, 200 W), the β-phase melting peak remains sharp, the melting curves have almost not changed. From Fig. 8, it is worth noting that the WAXD profiles of all samples in (a) and (b) are almost the same, indicating that during the 28-days cooling time, both α- and β-phase remain stable under room temperature. Figs. 7 and 8 suggest that the disappearance of β-phase melting peak in DSC curves occurs during the heating process. In order to observe what had happened during the 28 cooling days to β-iPP, samples with

Table 4
WAXD parameters of β-iPP under different intensities of ultrasonic irradiation.

UI intensity (W)	k_β(%)	*d*-spacing (angstrom)				*L*(nm)			
		$(110)_\alpha$	$(040)_\alpha$	$(130)_\alpha$	$(300)_\beta$	$(110)_\alpha$	$(040)_\alpha$	$(130)_\alpha$	$(300)_\beta$
0	68.3	6.273	5.261	4.766	5.531	10.8	14.1	11.4	22.5
50	81.5	6.279	5.250	4.776	5.497	9.9	13.6	8.2	16.6
100	79.6	6.308	5.323	4.790	5.545	9.3	11.9	5.0	13.5
150	75.7	6.305	5.285	4.791	5.542	9.3	12.8	4.4	19.6
200	75.5	6.318	5.329	4.794	5.549	9.8	13.7	5.8	16.8
250	75.8	6.328	5.339	4.806	5.556	8.9	13.0	6.0	14.5

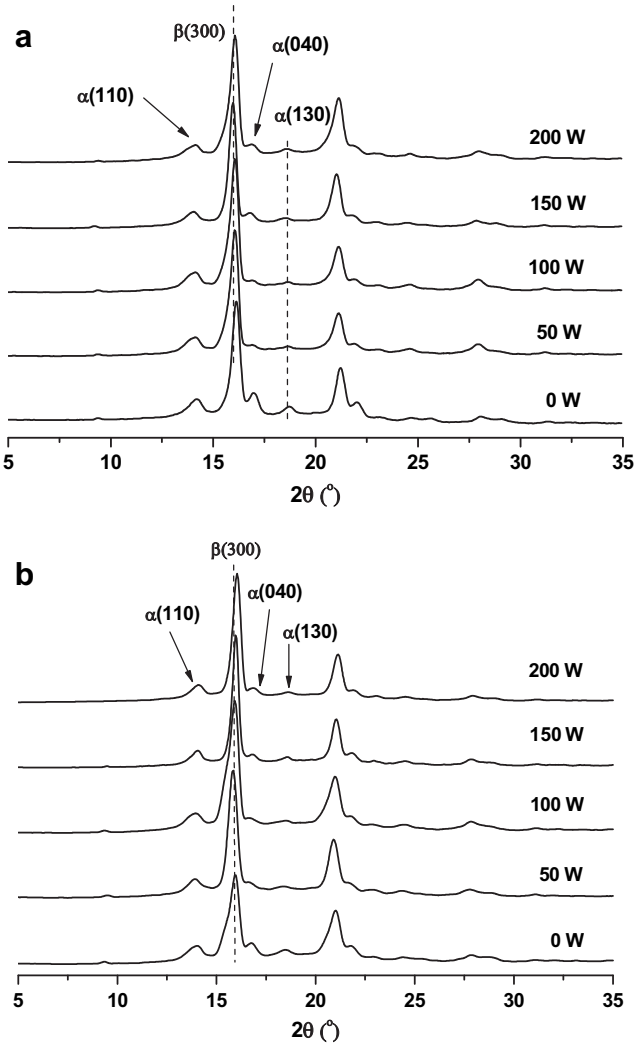

Fig. 8. (a) WAXD profiles of β-iPP samples newly prepared. (b) WAXD profiles of β-iPP samples cooled under room temperature 28 days after preparation.

(100 W, 150 W) and without (0 W) ultrasonic irradiation were prepared and the DSC measurement was taken every 7 days since preparation. The DSC results are shown in Fig. 9, the variations of β_c and $(1-\lambda)_\beta$, α_c and $(1-\lambda)_\alpha$ calculated from Fig. 9 are shown in Figs. 10 and 11, respectively, as a function of cooling time. Surprisingly, as the cooling time increases, for 0 W sample, β_c and $(1-\lambda)_\beta$ decrease gradually and vanish 28 days later; meanwhile, α_c and $(1-\lambda)_\alpha$ increase gradually. In contrast, for 100 W, 150 W samples, the β_c, $(1-\lambda)_\beta$, α_c and $(1-\lambda)_\alpha$ have almost not changed.

Figs. 7–11 clearly demonstrate that ultrasound greatly changes the crystallization and melting behavior of β-iPP. One possible mechanism concerning the melting memory effect of β-iPP is schematically illustrated in Fig. 12.

There exists some "locally ordered structure" within β-iPP melt. For samples without ultrasonic irradiation (0 W), after samples are cooled below T^*_R (i.e. 100–105 °C), the "locally ordered structure" can transform into evenly dispersed α-nuclei due to a self-nucleation process. It should be emphasized that it is the dispersed α-nuclei, not the "locally ordered structure", that can induce the $\beta\alpha$-recrystallization when the sample is heated. Moreover, based on the experimental results above, we believe that the formation of the evenly dispersed α- nuclei from "locally ordered structure" is a time-dependent process. When samples are newly prepared, the "locally ordered structure" has not transformed into the α-nuclei. When the samples are heated, without the evenly dispersed α-nuclei, the evident phase transformation does not happen (Fig. 7a); however, as the cooling time increases the amount of evenly dispersed α-nuclei formed by the "locally ordered structure" increases gradually (Figs. 7b, 9a, 10 and11), which then induces an

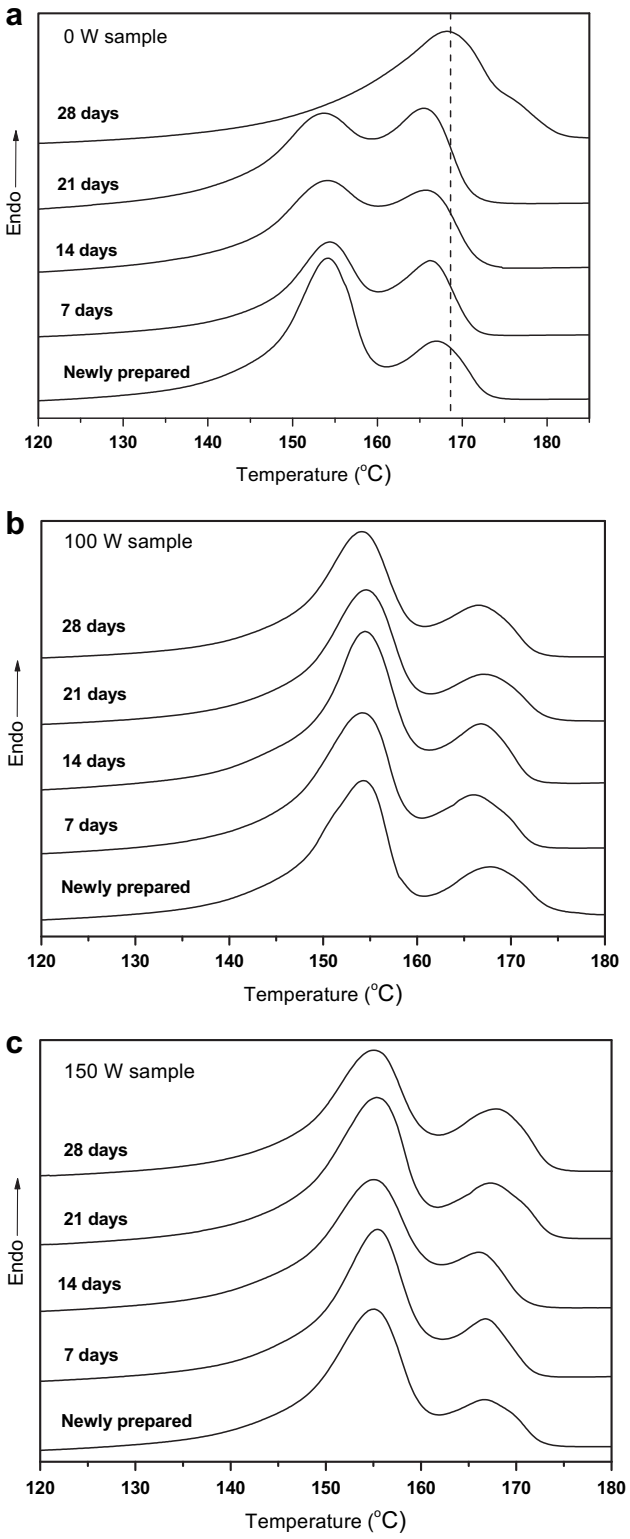

Fig. 9. DSC heating thermograms of β-iPP samples at different cooling time under room temperature after preparation. (a) 0 W. (b) 100 W. (c) 150 W.

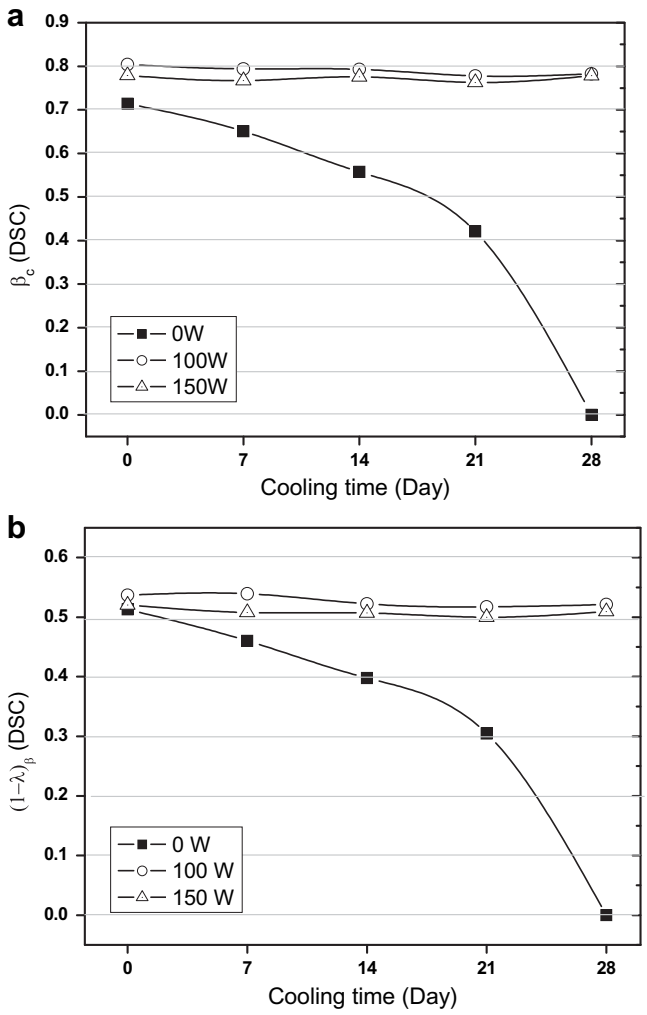

Fig. 10. (a) β_c as a function of cooling time under room temperature (b) The degree of crystallinity of β-phase $(1-\lambda)_\beta$ as a function of cooling time under room temperature. All the values were evaluated from DSC heating thermograms of β-iPP in Fig. 9.

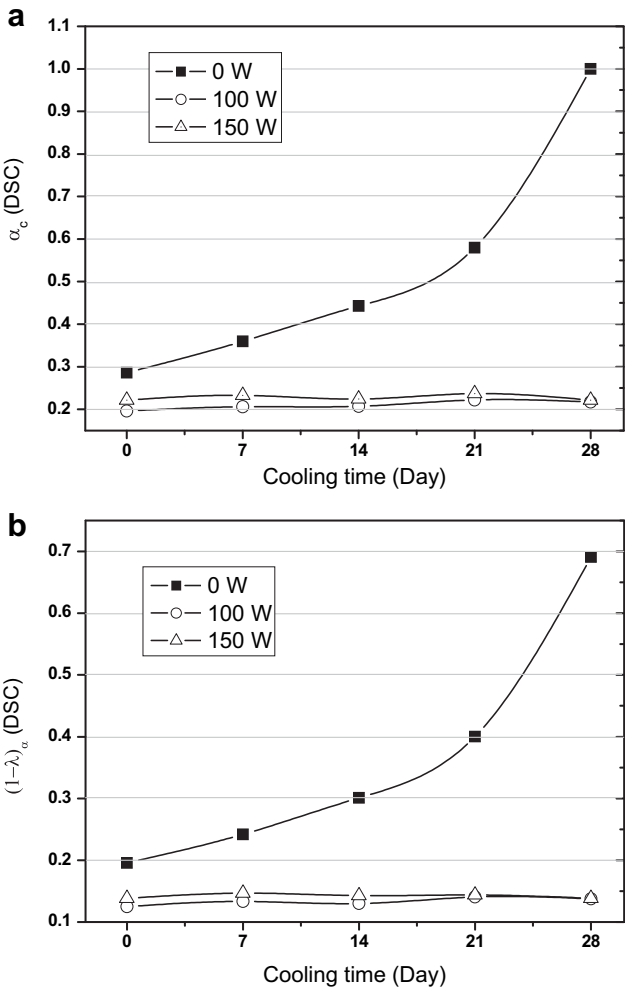

Fig. 11. (a) α_c as a function of cooling time under room temperature (b) The degree of crystallinity of α-phase $(1-\lambda)_\alpha$ as a function of cooling time under room temperature. All the values were evaluated from DSC heating thermograms of β-iPP in Fig. 9.

evident phase transformation when the sample is heated. In the DSC thermograms, the endotherm of the temporarily melting β-form, the exotherm of crystallization from molten amorphous into α-form and endotherm of the final melting of α-form are overlapped and finally make the β-phase melting peak unobservable 28 days later after preparation (Figs. 9a, 10 and 11).

For samples with ultrasonic irradiation, the strong stress, shatter and vibration effects of ultrasonic irradiation destruct the "locally ordered structure" within β-iPP melts, after cooling down, the amount of the remained "locally ordered structure" decreased prominently (Fig. 12). Consequently, the amount of the dispersed α-nuclei formed by the existing locally ordered structure due to the melting memory effect of α-crystals is not enough to induce an evident phase transformation during heating (Figs. 7a, 9b, and c). Ultrasonic irradiation inhibits the phase transformation from the metastable β-form to the stable α-form during heating and is an effective method to enhance the thermal stability of β-crystal during heating of β-samples.

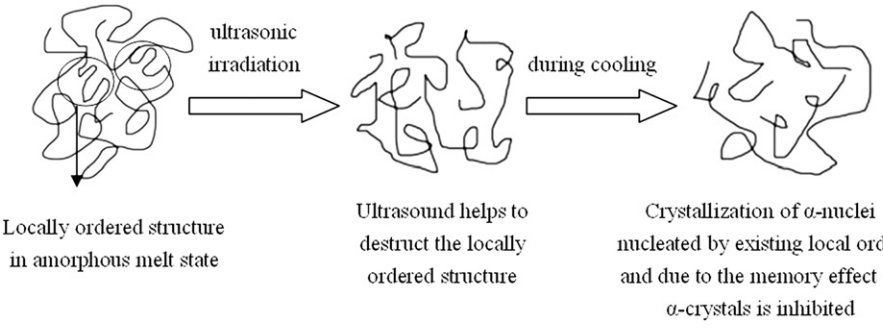

Fig. 12. Schematic representation of the influence of ultrasound on memory effect of β-iPP.

4. Conclusions

In the present wok, the changes of conformation and crystalline structure of iPP and β-iPP in the presence of ultrasonic irradiation, and the influence of ultrasound on the "melting memory effect" of β-iPP were investigated. The following conclusions can be drawn.

1. The degree of conformational order of iPP and β-iPP is decreased by ultrasonic irradiation. The intensities of the regularity bands at 998, 840, 1167 cm^{-1} corresponding to helical sequences with more than 5 monomer units decrease while the intensity of the regularity band at 973 cm^{-1} with 2–4 monomer units increases after ultrasonic irradiation, which might suggest that the iPP molecules prefer to fold into helical conformation with the shorter helical sequences (2–4 monomer units) rather than fold into the longer ones (more than 5 monomer units).
2. WAXD and DSC analysis indicates that for both iPP and β-iPP, after ultrasonic treatment, the degree of crystalline perfection decreases, the distribution range of crystalline perfection becomes wider, the crystalline particles pack looser and the crystallite size decreases, which might be related to the variation of conformation after ultrasonic irradiation. Moreover, ultrasound shows a selective effect on the growth of β-form, which encourages the growth of β-crystal.
3. The studies find that the transformation from "locally ordered structure" to α-nuclei is a time-dependent process. Ultrasound helps to destruct the "locally ordered structure" within β-iPP melt, erases the occurrence of melting memory effect and consequently inhibits the $\beta\alpha$-recrystallization to occur when the samples are reheated. The present work proves that ultrasonic irradiation is an effective method to destruct the "locally ordered structure" and inhibit the melting memory effect of β-iPP.

Acknowledgment

The financial support from the National Basic Research Program of China (2005CB623800) is greatly acknowledged.

References

[1] Isayev AI, Wong CM, Zeng X. SPE ANTEC tech. Papers 1987;33:207.
[2] Wong CM, Chen CH, Isayev AI. Polym Eng Sci 1990;30:1574.
[3] Isayev AI, Wong CM, Zen Z. Adv Polym Technol 1990;10:31.
[4] Isayev AI, Kumar Rishi, Todd M. Lewis Polym 2009;50:250.
[5] Levin VY, Kim SH, Isayev AI. Rubber Chem Technol 1995;69:104.
[6] Isayev AI, Yushanov SP, Chen J. J Appl Polym Sci 1996;59:803.
[7] Lemelson JUS. Pat. 4,288,398, 1981.
[8] Khamad SI, Popova EN, Salina ZI. Deposited Doc. (RUSS), VINITI 1984, 1829.
[9] Zerbi G, Ciampelli F, Zamboni VJ. Polym Sci 1963;C7:141.
[10] Kobayashi M, Akita K, Tadokoro H. Makromol Chem 1968;118:324.
[11] Kissin YV, Rishina LA. Eur Polym J 1976;12:757.
[12] Kissin YV, Tsvetkova VI, Chirkov NM. Vysokomol Soedin 1968;A10:1092.
[13] Kissin YV. Adv Polym Sci 1975;15:92.
[14] Miyamoto T, Inagaki H. J Polym Sci 1969;A2(7):963.
[15] Su ZQ, Wang HY, Dong JY, Zhang XQ, Dong X, Zhao Y, et al. Polymer 2007;48:870.
[16] Zhu XY, Yan DY, Yao HX, Zhu PF. Macromol Rapid Commun 2000;21:354.
[17] Zhu XY, Yan DY. Macromol Chem Phys 2001;202:1109.
[18] Zhu XY, Li Y, Yan DY, Zhu P, Lu Q. Colloid Polym Sci 2001;279:292.
[19] Zhu XY, Yan DY, Fang YP. J Phys Chem B 2001;105:12461.
[20] Padden Jr FJ, Keith HD. J Appl Phys 1959;30:1479.
[21] Uehare H, Yamazaki Y, Kanamoto T. Polymer 1996;37:57.
[22] Lotz B, Wittmann JC, Lovinger AJ. Polymer 1996;37:4979.
[23] Turner-Jones A, Aizlewood JM, Beckett DR. Makromol Chem 1964;75:136.
[24] Fujiwara Y. Colloid Polym Sci 1975;253:273.
[25] Varga J. J Therm Anal 1891;1989:35.
[26] Lotz B. Polymer 1998;39:4561.
[27] Cao Feina, Sadhan C. Jana Polym 2007;48:3790.
[28] Fujiwara Y. Colloid Polym Sci 1987;265:1027.
[29] Jain S, Goossens H, van Duin M, Lemstra P. Polymer 2005;46:8805.
[30] Varga. J. J Macromol Sci B 2002;41(4–6):1121.
[31] Zhang QX, Yu ZZ, Xie XL, Mai YW. Polymer 2004;45:5985.
[32] Zhao SC, Cai Z, Xin Z. Polymer 2008;49:2745.
[33] Yen Kai C, Woo Eamor M. Polymer 2009;50:662.
[34] Liu MX, Guo BC, Du ML, Chen F, Jia DM. Polymer 2009;50:3022.
[35] Varga J. J Therm Anal 1986;31:165.
[36] Varga J, Garzo G, Ille A. Angew Makromol Chem 1986;142:171.
[37] Cho K, Saheb DN, Choi J, Yang H. Polymer 2002;43:1407.
[38] Cho K, Saheb DN, Yang HC, Kang BI, Kim J, Lee SS. Polymer 2003;44:4053.
[39] Yamamoto Y, Inoue Y, Yakahashi H, Uehara H. Macromolecules 2007;40:2745.
[40] Cao YR, Li HL. Polym Eng Sci 2002;42:7.
[41] Cao YR, Xiang M, Li HL. J Appl Polym Sci 2002;84:1956.
[42] Marco C, Gomez MA, Ellis G. J Appl Polym Sci 2002;86:531.
[43] Li JX, Cheung WL, Demin J. Polymer 1999;40:1219.
[44] Scherrer P. Nachrichten Gesellschaft Wissenschaft Gottingan 1918;26:98.
[45] Kissin YV, Tsvetkova VI, Chirkov NM. Eur Polym J 1972;8:529.
[46] Varga J, Menyhard A. Macromolecules 2007;40:2422.
[47] Ziabickia A. Colloid Polym Sci 1994;272:1027.
[48] Alfonso GC, Ziabickia A. Colloid Polym Sci 1995;273:317.
[49] Zheng C, Zhang X, Dong X, Zhao Y, Wang D. Polymer 2006;47:7813.